ES3J1 Group 3 Report

Anya Akram, Edward Stanley, Favour Rabiu, Matt Brooks, Nojus Plungė

May 3, 2023

Question 1

The output produced by the motor is not smooth, so to obtain its model that can be analysed using control system theory, a filter needs to be designed.

The filter (and thus, the model) tuning was done according to the brief. The process followed the steps outlined below:

1. The filter coefficient was set to the simplest low-pass transfer function $\frac{1}{0.1s+1}$ to start smoothing the motor output, obtained by applying the step input. An example filter performance is shown in *Figure 1.*

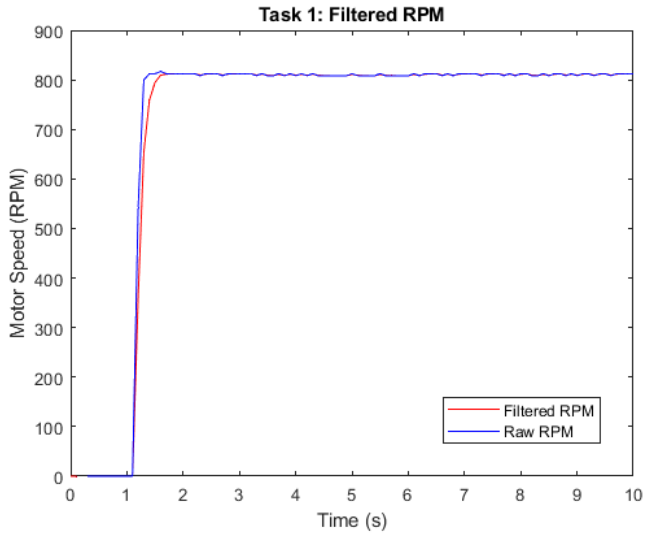

Figure 1: Low-pass filter's impact on the signal.

2. The motor circuit, as set up in the brief, was assembled; the motor and Arduino were connected to the circuit and a link was established to the Simulink workspace.
3. The motor was run using the MATLAB hardware add-on. The signal could be traced as going from the workspace input, through the PWM converter block and into the Arduino. The PWM signal generated by the Arduino then propagated through the circuit to power the motor, which had its encoder linked to the Arduino – this signal was then converted into motor revolutions per minute (RPM) in the workspace and the obtained results were designated as the output. The input into the system and the output of the motor (in RPM) was saved to the workspace for further analysis.
4. System Identification Toolbox (SIT) was used, with the input being the signal prior being processed by the PWM block and the output being the motor's RPM.
5. In SIT the analysis was set for the transfer function to have no zeroes and one pole – this was identified by inspection, using the unfiltered transfer function output, as the step input produced a first order response.

6. The obtained transfer function was scaled by dividing both the numerator and the denominator by the step time ($T_s = 0.1$).
7. The obtained transfer function was plotted against the unfiltered motor output to verify the model accuracy. If proven significantly inaccurate, the design process was repeated until a fitting filter that produced a smooth transfer function was obtained.

The resulting transfer function's step response is shown in *Figure 2* (titled as "Computed (SIT)").

An alternative method for tuning the transfer function was also explored, as the steady-state value of the produced function did not exactly match the motor output on the graph. The new tuning approach was found in [1] and was executed in the following steps:

1. Steps 1-3 were repeated from the previous method: a simple low-pass filter was set up, the motor circuit was assembled and the motor response to a step input was saved to the workspace.
2. Find the maximum gain reached by the output. This is regarded as the absolute – or steady-state – gain. The value recorded was 834.
3. The time constant for the response was calculated. This was defined as the time to reach 63.2% of the steady-state value. In this case, a value of 528.76 RPM needed to be reached. The time to reach this value was calculated to be 1.185s. As the step was applied at $t = 1$ s, the time constant was therefore $\tau = 1.185 - 1 = 0.185$s.
4. Using the standard first order transfer function model:

$$G(s) = \frac{Y(s)}{X(s)} = \frac{K}{\tau s + 1}$$

and substituting the values calculated, a final transfer function was obtained:

$$G(s) = \frac{834}{0.185s + 1}$$

The resulting transfer function's step response is shown in *Figure 2* (titled as "Graphical").

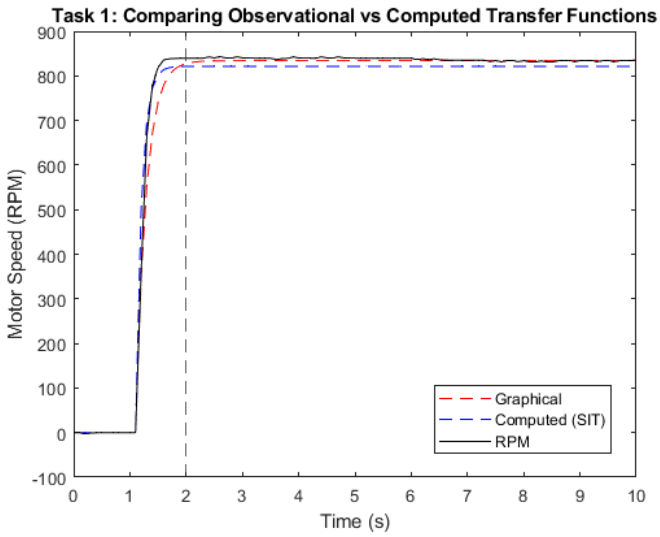

Figure 2: Step responses of transfer functions

The performance of the both functions were compared by calculating the mean-squared errors (MSEs) ϵ for each in a given timeframe:

- Transient-state error ($0 < t <= 2$): the computed transfer function MSE was found to be $\epsilon_{ts-c} = 3.77 \times 10^4$, while the graphically-found transfer function's MSE was found to be $\epsilon_{ts-g} = 1.66 \times 10^4$. Overall, the MSE was 227% higher using the SIT-calculated transfer function than the graphically-calculated transfer function.
- Steady-state error ($t > 2$): the SIT-calculated transfer function's MSE during the steady-state operation was found to be $\epsilon_{ss-c} = 243.0$ and the graphically-found transfer function's MSE during steady-state operation was $\epsilon_{ss-g} = 17.6$. Overall, there was a 1381% increase in the MSE value of the SIT-calculated transfer function compared to the graphically-calculated transfer function.
- Overall error ($t > 0$): the total MSE for the SIT-calculated transfer function was $\epsilon_{T-c} = 3.94 \times 10^3$ while the overall MSE for the graphically-calculated transfer function was $\epsilon_{T-g} = 1.66 \times 10^3$. Overall, the total MSE was 237% larger for the SIT-calculated transfer function than for the graphically-generated function.

Having evaluated the errors, further tasks were performed using the graphically-generated transfer function, as it outperformed the SIT-generated function for both transient and steady-state parts of the step response.

Upon observation of the motor function, the motor had a 0.1 second delay, thus the transfer function needed to be multiplied by $e^{-0.1s}$ to account for this delay.

The final design allowed for the produced output to be a smooth 1st order response, which enabled further analysis and tuning of the system in the subsequent tasks.

The open-loop Simulink model used to obtained the results discussed in this section is shown in *Figure 3*.

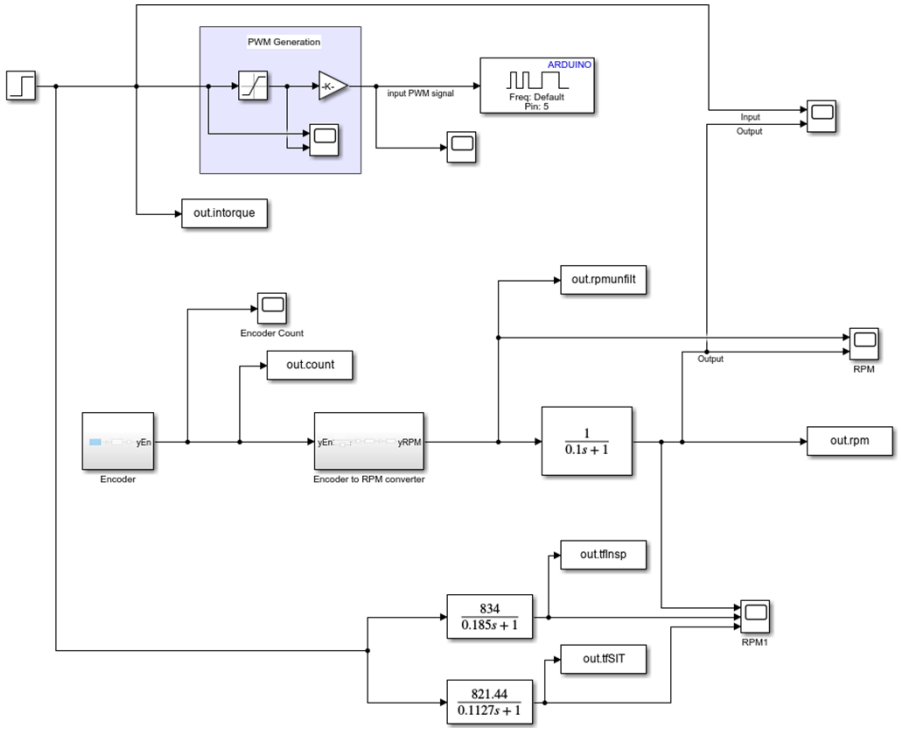

Figure 3: The model used to obtain the measurements

Question 2

Using the transfer function obtained in Question 1, closed-loop analysis of the system was used to obtain the required constants for proportional-integral (PI) control. The Ziegler-Nichols

method was chosen due to its ease of implementation.

An initial PI system was created with K_p and K_i both set to zero. K_p was slowly increased in increments of 0.001, until consistent oscillations were produced in response to a step input. At $K_p = 0.016$, constant oscillations occurred. The system response using the oscillatory K_p is shown in *Figure 4*.

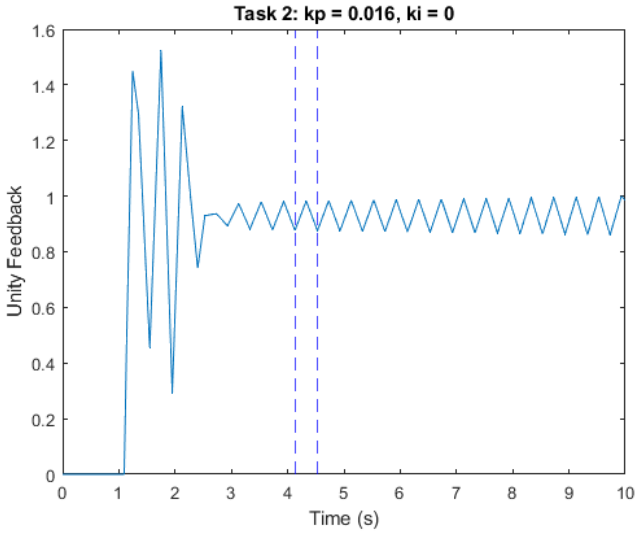

Figure 4: The oscillatory graph used in the Ziegler-Nichols tuning

The peak-to-peak time was measured to obtain the ultimate time period $P_u = 0.407$ s, giving an ultimate gain of $K_u = 0.016$.

The Ziegler Nichols tuning equations were applied to obtain the controller values of K_p and K_i. The response of the system using the calculated K_p and K_i is shown in *Figure 5*. An important consideration is that the produced K_i value produced unstable step responses, so it was scaled down by an order of magnitude of two to obtain a stable plot.

$$K_p = 0.45 * K_u = 0.45 * 0.016 = 0.0072$$
$$K_i = 0.83 * P_u = 0.83 * 0.407459 = 0.338$$

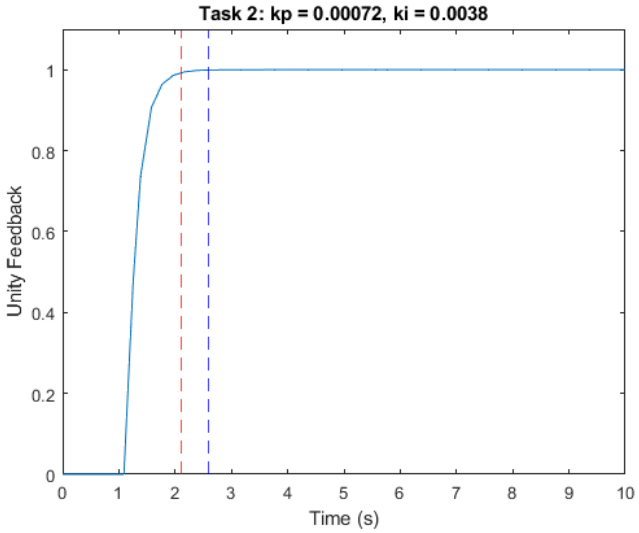

Figure 5: The step response with scaled K_i, obtained from Ziegler-Nichols method.

The K_p and K_i values were then adjusted by multiplying both by the sample time $T_s = 0.1$s to

produce $K_p = 0.00072$ and $K_i = 0.0338$.

Upon testing these values, the output displayed violent oscilations. Hence, K_i was once again scaled down by a magnitude of 10. When implemented, this produced the step response depicted in *Figure 6*.

Whilst the settling time was within the required parameters, the peak time exceeded the 1 second requirement, hence K_i was increased to 0.005.

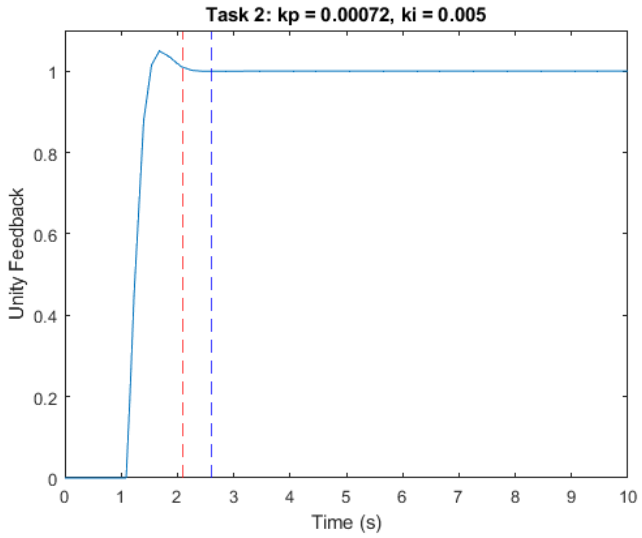

Figure 6: Step response of adjusted K_i to meet the response requirements.

Finally, for open loop analysis, a step input of magnitude 1 was used. However, in a closed-loop system a reference speed is required. Hence, a block of gain $K = 834$ (the steady-state gain, observed in open loop analysis) was used to scale the output. The step response of the tuned model is shown in *Figure 7*.

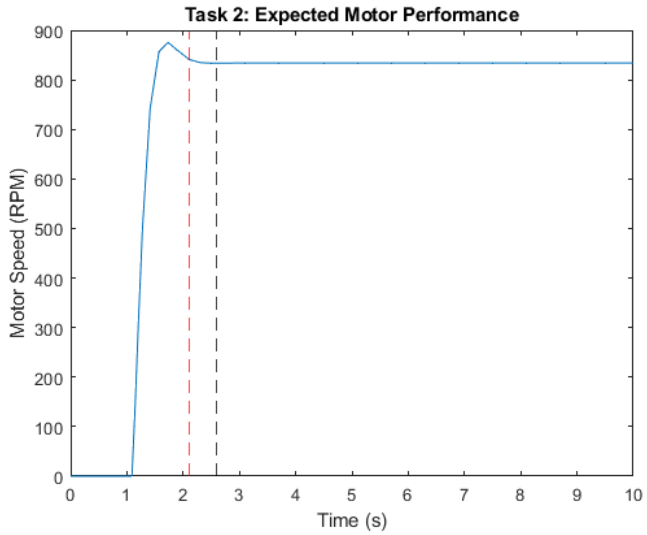

Figure 7: Step response, expected from the motor.

The Simulink model that was used to generate the plots is presented in *Figure 8*.

Question 3

After having the simulated model working, the next step was to integrate it on the Arduino to check against the posed requirements and physical constraints.

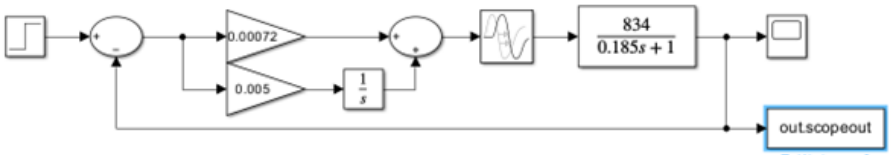

Figure 8: The model used to obtain the plots.

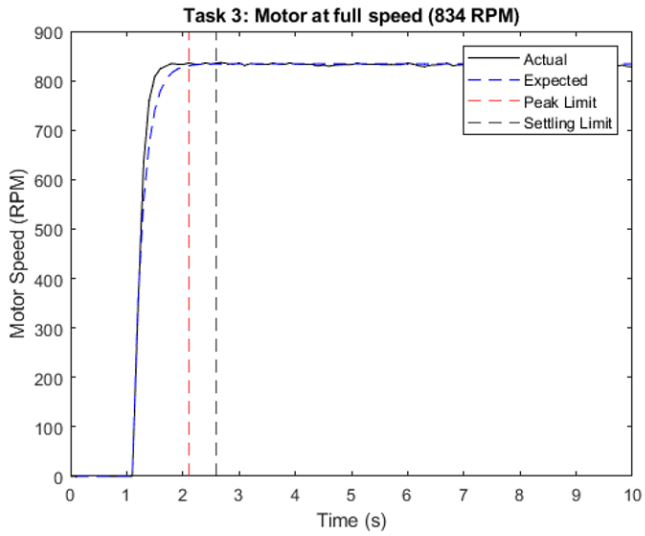

Figure 9: The step response of the motor at full speed with a PI controller.

As observed *Figure 9*, the response in simulation was very close to the actual response generated by the motor. The response stabilised well within the peak limit and settling time limit and showed no overshoot of the steady-state value. In fact, it reached the steady-state faster than the simulated response, with a settling time of around 0.8 seconds, compared to 1.28 seconds for the simulated response. This confirmed that the chosen values for the PI controller were accurate and produced the desired results. In order to further verify the accuracy of the controller, different motor speeds were tested. These produced more varied results as shown in *Figures 10 and 11*.

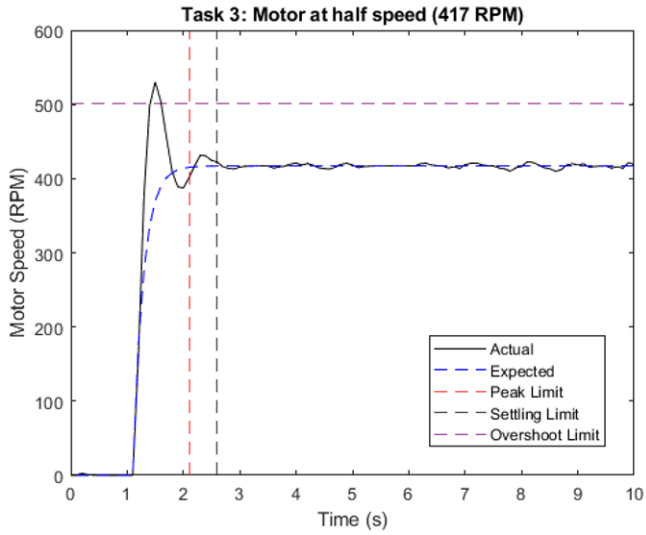

Figure 10: The motor's response to a half step input.

Comparing the performance of the motor to the simulated response with PI control applied, there appeared to be significant overshoot when run at half speed which was not present in the full speed response. As shown in *Figure 10*, a peak value of 524 RPM was reached, which

exceeded the overshoot limit of 20%, and only just stabilised within the settling time limit. This proved that at lower speeds, the PI controller did not perform as robustly in real-life as it did in simulation, and showed that there was still room for improvement of the controller. To confirm these findings, the motor was also tested at a quarter speed (*Figure 11*).

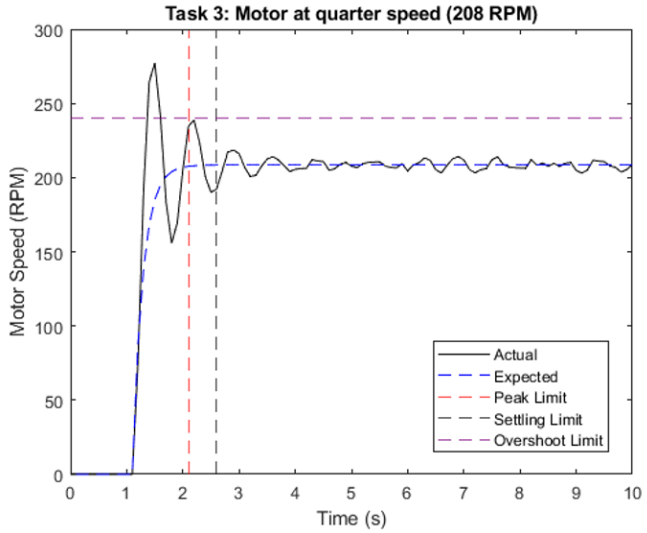

Figure 11: The motor's response to a full step input.

The results in *Figure 11* show that the PI controller did not meet any of the specifications when the motor was run at a quarter speed. The overshoot of 275 RPM was far too high, and showed much more oscillation before a steady-state was eventually reached. This was far from the predicted response gained using the transfer function, and prompted exploration into why these discrepancies might have occurred.

The primary reason for a difference between the performance of the motor in simulation and in the real-world is due to the fact that the mechanical properties of the device are difficult to model in simulation. Electrical properties can be modelled with greater accuracy, but parameters such as friction which could act against the rotor torque, thereby reducing the motor speed and limiting the current through the coils of the motor, is much more difficult to predict. Typically, friction effects are less noticeable at higher speeds, and have a much greater impact at lower speeds. Coulomb friction and viscous friction are two such examples. Coulomb friction opposes motion and is always present, and is independent of velocity. Viscous friction is dependent on velocity, and therefore increases as velocity increases [2].

Additionally, non-linearities inherent in the behaviour of the motor are assumed to be negligible when designing the model and generating a linear transfer function. This is because it is more convenient and is often sufficient for conventional control problems. However, this non-linear behaviour in certain regions of operation, make the PI controller difficult to tune for real-world usage, as the effects of friction are highly varied and dependent on parameters which are not easily modelled. Once such example of this is demonstrated well by the graphs at lower motor speeds, where static friction is particularly challenging to overcome. Static friction is an effect which occurs when a component has been inactive for a certain period of time, and therefore requires a greater force to start the relative motion than the force which is required to sustain this motion. This effect is demonstrated well by the longer settling time shown at lower motor speeds than that of the motor running at full speed, proving that more force was required to start the motor and overcome the static friction [3].

Question 4

To compensate for some of the controller weaknesses encountered in previous chapter, a variety of techniques were explored – some of which are discussed below. The techniques were used individually and not coupled to explore their effect on the PI controller.

PID Control

The PI controller performed optimally at full speed, however it showed more variation when the motor was run at half speed and quarter speed with regard to overshoot and oscillations in the transient response. This showed that further tuning was necessary, thus PID control was explored as a method to overcome these shortcomings. The intention of adding the derivative controller was to reduce overshoot, as derivative gain is proportional to the rate of change of the process variable, so acts to reduce output when the process variable is increasing quickly. The tuning of this gain parameter followed an offline trial and error approach, as values could be tested more quickly and safely than the online equivalent. Once a suitable order of magnitude was determined in simulation, more specific values were tested using the motor. The ideal order of magnitude for the derivative gain was found to be 10^{-5}, thus the gain was slowly increased from 0.00001 in increments of 0.000005, with the motor running at half speed until the optimal response was reached. The K_i and K_p values were left unchanged, and this resulted in a K_d value of 0.00004 producing the best response at lower motor speeds.

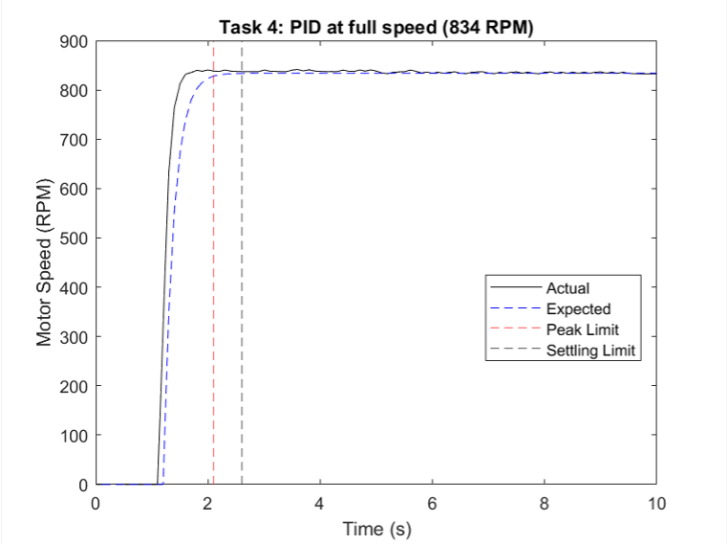

Figure 12: The motor's response at full-speed, using PID.

With PID control applied, the step response in *Figure 12*. As shown by the graph, there is no overshoot of the steady-state value, and the settling time of 884 ms falls adequately within the settling time limit. This is very similar to the response seen using PI control, and confirms that the PI values chosen for this controller were correct.

The graph in *Figure 13* shows vast improvement in the desired areas, with a settling time and overshoot within the predetermined limits. The response shows an overshoot of just under 20%, as it reaches 499 RPM, and just settles within the required 1.5s. Although this controller only just fulfils the requirements, any corrections to individual aspects appeared to come at the expense of deteriorating other areas of the response. For example, although increasing the derivative gain effectively reduced overshoot, it resulted in greater oscillations in the steady-state part of the response, and a slightly longer settling time. For this reason, the values of K_p, K_i and K_d were chosen such that the controller remained just within the overshoot and settling time limits, whilst maintaining a smoother steady-state response at the desired RPM.

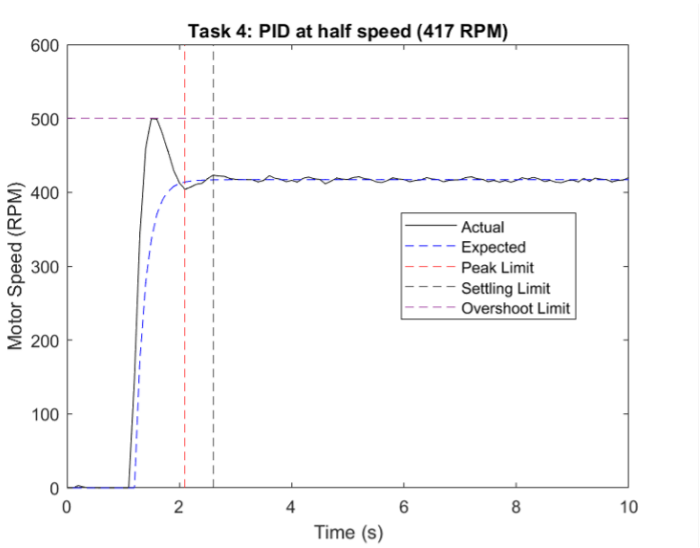

Figure 13: The motor's response at half-speed, using PID.

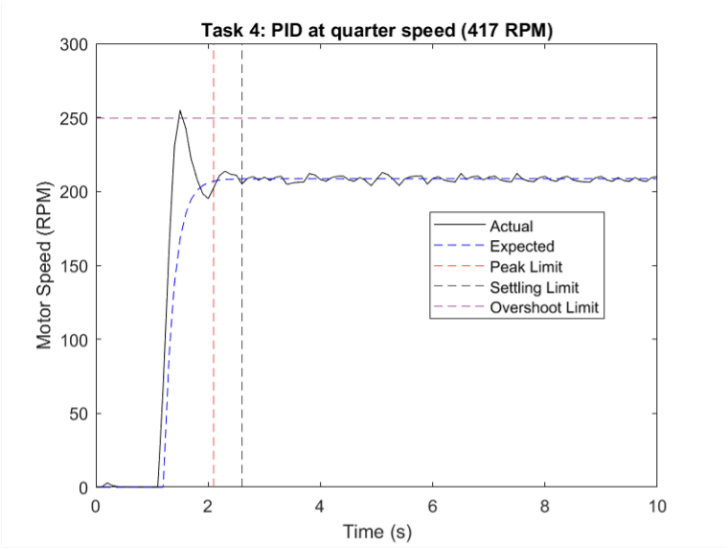

Figure 14: The motor's response at quarter-speed, using PID.

In *Figure 14*, the step response using PID control again showed improvement to the PI control output, which displayed greater overshoot and oscillated much more in the transient part of the response than the result using PID control. A peak speed of 261 RPM was reached, which was just beyond the desired 20% overshoot limit, and the same was true of the settling time, which appeared to occur at around 1.5 s. Similarly to the results at half speed, a compromise between the optimisation of these factors was reached, with the Kp, Ki and Kd values chosen such that overshoot was limited while keeping oscillations in the steady-state to a minimum, and remaining just within the settling time bounds.

Model Predictive Control Integration

To further improve upon the controller design for our group task, we decided to utilise the Model Predictive Control (MPC) method in Simulink, this was obtained by installed the Model Predictive Control Toolbox in MATLAB.

Model Predictive Control systems operates by using numerically minimising a cost function of a plant provided to it, to generate output predictions over a finite time horizon, continuously iterating over time [4].

A typical MPC system contains an input-output system to control, in this instance it's the DC

powered motor where the input is voltage & output is torque.

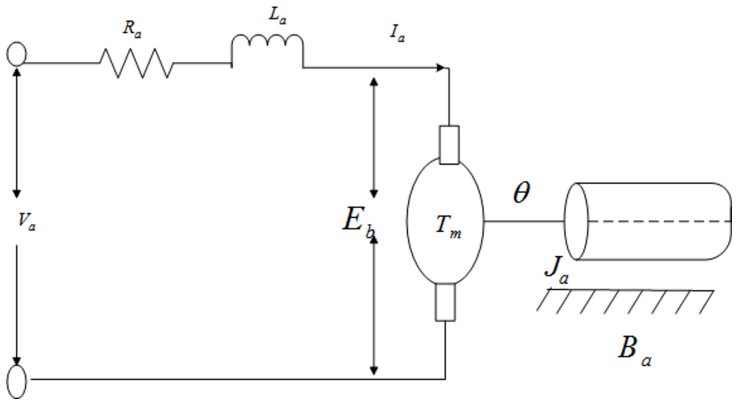

Figure 15: DC motor circuit schematic [5]

MPC is an improvement as it computes predicted future output values and computes a predicted future error as input for its cost-function optimizer. The optimizer will produce new inputs for the model and feed the model the input value that produces the least error. The cost-function optimizer does this by enforcing the constraints of the system (the first order equations derived from the transfer function that represents the DC motor system offline) [6].

This reduces overall control effort of the system, in comparison to traditional PI/PID controllers and thus better overall responses, regarding peak time, settling time & percentage overshoot. The parameters used in the MPC and the response parameters are summarised in *Table 1* and *Table 2*.

Ts	**PredictionHorizon**	**ControlHorizon**	**Weights.ManipulatedVariables**
0.1	1	2	0.5

Table 1: The parameters used for MPC set-up.

Mode	**Settle Value, rpm**	**Peak Value, rpm**	**Overshoot, %**	**Peak Time, s**	**Settling Time, s**
Full-Speed	834	839	0.6	0.7	0.7
Half-Speed	538	597	11.0	0.4	1.2
Quarter-Speed	265	351	32.5	0.3	1.8
Tenth-Speed	48	64	33	1.4	2.9

Table 2: The parameters used for MPC set-up.

The responses associated with the presented values are depicted in *Figure 16* and *Figure 17*.

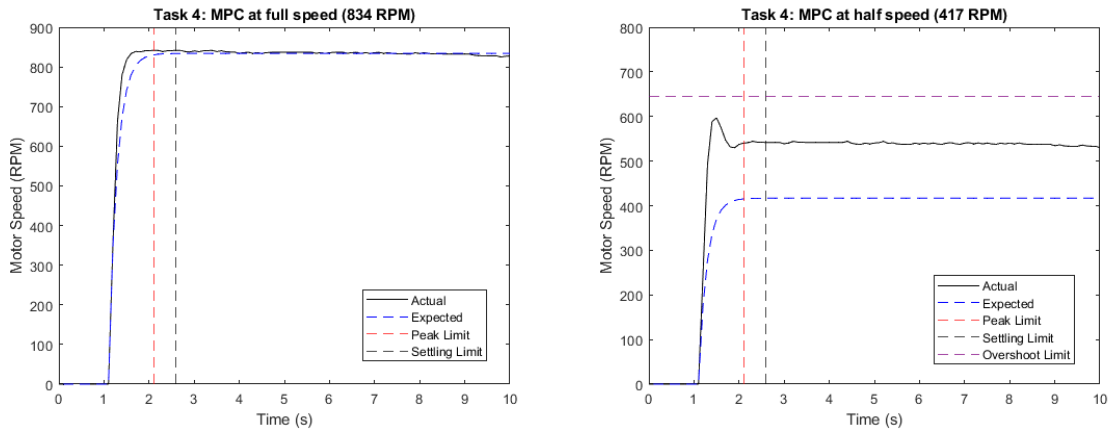

Figure 16: The motor's response at full-speed (left) and half-speed (right), using MPC.

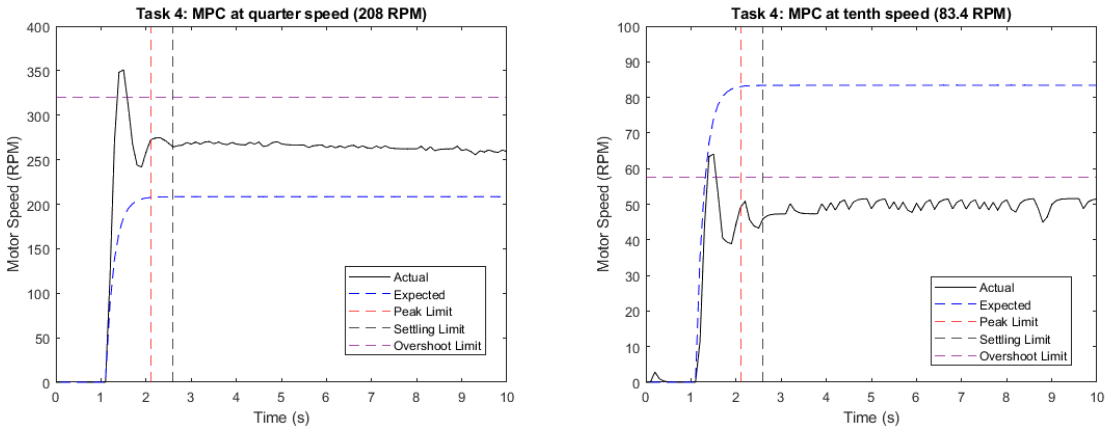

Figure 17: The motor's response at quarter-speed (left) and tenth-speed (right), using MPC.

References

[1] "Control Tutorials for MATLAB and Simulink - PI Control of DC Motor Speed — ctms.engin.umich.edu," https://ctms.engin.umich.edu/CTMS/index.php?aux=Activities_DCmotorB, [Accessed 01-May-2023].

[2] I. Virgala and M. K. Peter Frankovský, "Friction effect analysis of a DC motor," *American Journal of Mechanical Engineering*, vol. 1, no. 1, pp. 1–5, Jan. 2013. [Online]. Available: https://doi.org/10.12691/ajme-1-1-1

[3] "Study of Nonlinear Behavior of DC Motor Using Modeling and Simulation — ijsrp.org," http://www.ijsrp.org/research-paper-0313.php?rp=P15939, [Accessed 01-May-2023].

[4] M. Nikolaou, "Model predictive controllers: A critical synthesis of theory and industrial needs," in *Advances in Chemical Engineering*. Elsevier, 2001, pp. 131–204. [Online]. Available: https://doi.org/10.1016/s0065-2377(01)26003-7

[5] L. Aloo, P. Kihato, and S. Kamau, "Dc servomotor-based antenna positioning control system design using hybrid pid-lqr controller," *European International Journal of Science and Technology*, vol. 5, 04 2016.

[6] "12.3: MIMO using Model Predictive Control — eng.libretexts.org," https://eng.libretexts.org/Bookshelves/Industrial_and_Systems_Engineering/Chemical_Process_Dynamics_and_Controls_(Woolf)/12%3A_Multiple_Input_Multiple_Output_(MIMO)_Control/12.03%3A_MIMO_using_model_predictive_control, [Accessed 02-May-2023].